



Development of a High Throughput in Vitro Protein Localization Assay to Characterize Potentially Pathogenic Genetic Variants Associated With Retinitis Pigmentosa

Citation

Wan, Aliete L. 2016. Development of a High Throughput in Vitro Protein Localization Assay to Characterize Potentially Pathogenic Genetic Variants Associated With Retinitis Pigmentosa. Master's thesis, Harvard Extension School.

Link

<http://nrs.harvard.edu/urn-3:HUL.InstRepos:33797382>

Terms of use

This article was downloaded from Harvard University's DASH repository, and is made available under the terms and conditions applicable to Other Posted Material (LAA), as set forth at

<https://harvardwiki.atlassian.net/wiki/external/NGY5NDE4ZjgzNTc5NDQzMGIzZWZhMGFIOWI2M2EwYTg>

Accessibility

<https://accessibility.huit.harvard.edu/digital-accessibility-policy>

Share Your Story

The Harvard community has made this article openly available.
Please share how this access benefits you. [Submit a story](#)

Development of a High Throughput *In Vitro* Protein Localization Assay
to Characterize Potentially Pathogenic Genetic Variants Associated with
Retinitis Pigmentosa

Aliete Langsdorf Wan

A Thesis in the Field of Biology
for the Degree of Master of Liberal Arts in Extension Studies

Harvard University

November 2016

Abstract

Retinitis pigmentosa is a disease comprised of a group of retinal degenerations (RD) that affects about 1/4,000 people worldwide (Wang, 2014). Currently, there is no cure for RP, and studying the disease is difficult because it is so genetically and phenotypically heterogeneous and because investigation of the retina *in vivo* is necessarily invasive. The advance of next generation sequencing (NGS) has allowed for great inroads into the genetic investigation of this disease. Here we describe the development of a flexible *in vitro* assay based on protein surface expression to identify potentially pathogenic genetic variants of unknown significance (VUS) discovered via NGS. The assay relies on the methods of plasmid transfection, immunofluorescence, fluorescence activated cell sorting (FACS) and NGS. By creating a library of *Rhodopsin (RHO)* variants to test our system, this work serves as proof of concept that we are able to efficiently pool and then deconvolute a mixture of cells transfected with different variants into categories based on protein localization. This assay could theoretically be used to test VUS in a variety of genes related to RP and beyond, thus facilitating not only the characterization of VUS discovered through NGS, but also influencing the development of possible future therapies.

Acknowledgments

I am grateful for the institutions that not only trained me on the job, but also contributed to my intellectual growth at Harvard: Boston Biomedical Research Institute, Dana-Farber Cancer Institute and Massachusetts Eye and Ear Infirmary. I am also thankful to the people who lent their technical expertise to the realization of this project, especially David Dombkowski. I am also thankful for the many people who have helped me grow as a scientist throughout my career. To Dr. Xingbin Ai and Dr. Jennifer Chen: Thank you for training me in good lab habits and teaching me how to be a researcher. Thank you to my thesis director Dr. Qin Liu without whom I could not have submitted this work and to my thesis advisor Dr. James Morris for his help with manuscript preparation. Thank you most especially to Dr. Jason Comander, my thesis advisor and boss, who has inspired and challenged me to be a critical and careful scientist. I am a better researcher because of your example.

Thank you to my family and friends who have encouraged me in my studies in the years leading up to this thesis. Thank you to my parents for instilling in me a love of learning. Thank you, Henry, for helping me finish strong and with a new last name. I love you. Finally, I am thankful to God to have had the ability and opportunity to spend time learning from and about His creation, and hope to contribute to the body of scientific research in a manner that brings honor to His name.

Table of Contents

Acknowledgments.....	iv
List of Tables.....	vii
List of Figures.	viii
Introduction.....	1
Clinical Manifestation.....	1
Genetic Signature.....	3
Cellular Manifestation and Pathology of RP.....	4
Mechanism of Photoreceptor Cell Death in RP.....	6
Rhodopsin’s Role in Vision: A closer look.....	6
Disease Model Systems.....	9
Current State of RP Therapy.....	11
Significance.....	12
Materials and Methods.....	13
Creation of Library.....	13
Mammalian Cell Culture.....	15
Transfection for Microscope Viewing and Rating.....	15
Immunocytochemistry for Microscope Viewing and Rating.....	15
Transfection for FACS.....	16
Flow Cytometry.....	17

<i>RHO</i> Plasmid Extraction from Sorted Cells.....	18
<i>RHO</i> PCR Amplification.....	18
Results.....	19
Discussion.....	24
Appendix.....	30
References.....	48

List of Tables

Table 1	<i>Rhodopsin</i> variant table.....	36
Table 2	Protein localization assay aids in characterization of <i>RHO</i> VUS.....	45

List of Figures

Fig.1	Normal versus RP vision.....	30
Fig.2	Normal versus RP fundus.....	31
Fig.3	Schematic of eye anatomy.....	32
Fig.4	Light signaling cascade in rod outer segment.....	33
Fig.5	Classes and locations of known <i>Rhodopsin</i> mutants in 2005.....	34
Fig.6	<i>RHO</i> expression plasmid used in transfections.....	35
Fig.7	Rhodopsin surface expression in transfected cells.....	38
Fig.8	Immunocytochemistry compared to standard FACS assay.....	39
Fig.9	Validating surface expression assays.....	41
Fig.10	Results of standard FACS assay for variant cohort.....	42
Fig.11	Overlay of standard FACS assay for WT and P23H with gates shown	43
Fig.12	Standard FACS assay correlates with NGS read analysis of sorted cells.....	44
Fig.13	Effect of cell preparation on phenotype readout by FACS.....	47

Chapter I

Introduction

The following is an introduction into the clinical, cellular and genetic understandings of retinitis pigmentosa.

Clinical Manifestation

Retinitis pigmentosa (RP) is a congenital disorder with disease indications probably present at birth, but not usually noticeable to the patient until about the second decade of life. For many, symptoms first become noticeable when learning to drive during adolescence. Patients often arrive at the doctor's office because of noticeable decreased peripheral vision and loss of night vision (nyctalopia), a hallmark of Stage I RP. Progression can be slow, but as the disease runs its course over the coming decades, the loss of sight progresses to Stage II - pronounced tunnel vision - until eventually rendering the patient legally blind by middle age (Stage III). (See Figure 1.)

Besides the symptoms experienced by the patient, there are also classic indications of the disease that are observable by an ophthalmologist. Fundus photographs of the back of the eye, for instance, will reveal a characteristic pattern of bone spicule-like pigmentation in the peripheral retina, as well as thinning of blood vessels. (See Figure 2.)

The pigmentation seen in RP fundus photos is in fact the dark outermost layer of the retina, termed the retinal pigment epithelium (RPE), showing through the rest of the neural retina; in a healthy eye, the inner retina is thicker and the RPE does not show through. (See Figure 3 for eye anatomy.) Besides fundus photos, an electroretinogram (ERG) is also performed to confirm a diagnosis of RP. This test, done by attaching electrodes to the cornea, records the electrical response of the photosensitive cells of the retina to a light stimulus. In response to light stimulus, both types of photoreceptors, rods and cones, do not respond normally in RP.

Though these hallmark symptoms unite RP into one category, the disease is still better understood as a collection of diseases with a similar outcome. For this reason, predicting prognosis can be very difficult in the absence of genetic screening. In fact, in 2002, a longitudinal study was performed which established that there is no true “average” rate of visual decline for an RP patient. The study, which followed a subset of RP patients whose DNA harbored mutations mapped to the *Rhodopsin (RHO)* gene, found that, though all the patients had mutations in the same gene, the rate of progression still varied among patients. However, it was found that the location of the mutation within the gene, rather than simply the gene itself, did correlate to a faster or slower rate of progression of the disease (Berson, 2002). This study focused only on patients with *RHO* mutations; the heterogeneity of phenotype has an even wider range when mutations from any of the other 50 genes and 3,100 mutations reported to be associated with RP are taken into consideration (Daiger, 2013). Furthermore, it has been shown that, at least in mice, genetic background can greatly influence the rate of progression of disease for animals with the exact same genetic lesion, as seen in studies using the *Prom1*^{-/-}

genetically engineered mouse model (GEMM) of RP (Dellell, 2015). Extrapolating from this data suggests that in humans as well, confounding genetic factors may exacerbate or ameliorate symptoms even when people harbor the same RP-associated mutation.

Genetic Signature

One way of categorizing the several forms of RP is by genetic inheritance. Although 40-55% of forms cannot be traced genetically, for the remaining cases it is estimated that about 20% are autosomal recessive, 20-25% are autosomal dominant and 10-15% are X-linked (Wang, 2005). There are also several syndromes with symptoms extending beyond vision loss, but which include RP as a hallmark: Usher syndrome, Leber's congenital amaurosis, rod-cone disease, Bardet-Biedl syndrome, Best disease, choroideremia, gyrate-atrophy, Stargardt disease and Refsum disease. However, the names of these syndromic forms are being phased out in favor of calling each disease by the gene associated with it, as "Best-1 associated RP" instead of "Best disease".

Since this disease has so many potential genetic causes, clinical diagnosis is often confirmed by genetic testing. It has been established that the two genes most commonly involved in RP are *Rhodopsin (RHO)* and *Retinitis Pigmentosa GTPase Regulator (RPGR)*. Mutations in *RHO* account for up to 40% of all cases of autosomal dominant RP (adRP) (Berger, 2015). Furthermore, the P23H mutation, in which, due to a point mutation, the 23rd amino acid in the peptide chain at the N-terminal of the protein is switched from a proline to a histidine, has been shown to be the most common *RHO* mutation in North American populations (Chen, 2014 & Berson, 2002). This mutation is

used in these experiments as a positive control for the development of a VUS characterization assay.

Cellular Manifestation and Pathology of RP

The retina is a complex tissue made up of intricately layered and intercalated cells where light entering through the pupil is received by photo-sensitive cells and eventually electrical signals sent to the brain to induce the phenomenon of vision. Photoreceptors, the focus of this project, lie in the outermost layer of the retina and are the light-sensitive cells.

There are two types of photoreceptor cells in humans: rods and cones. Rods, which comprise 97% of the all photoreceptors in the human retina (Wert, 2014), respond to light and dark only (they are not sensitive to color) and are located throughout the retina, but at the highest density just peripheral to the fovea – the center of the field of vision. Cones, which detect color, are also found throughout, but in an opposite pattern to the rods: they are scarce everywhere but the fovea, and there they are present at an extremely high density, thus bestowing the best visual acuity to whatever is in focus. Rods and cones differ not only in function, but also in shape. Both are specialized ciliated cells, where the specialized cilia, called outer segments (OS), are filled with membranous discs that house pigment proteins that are light-sensitive. In the rod the outer segments are longer and more rod-like, while in the cone they are shorter and tapered (Figure 3). In addition, the discs in cone OS are contiguous with the cell membrane, whereas in rod OS they are separate from the cell membrane. In any case, for both rods and cones, the OS

are intercalated with a layer of supportive cells known as the retinal pigment epithelium (RPE), which delivers nutrients and exchanges waste with the photoreceptors, and which are dark in color in order to absorb extra light and reduce glare. The RPE also has a specialized function in which it phagocytoses the OS of the photoreceptors each day. Therefore, the outer segments, and the color-sensitive pigments they house, must be regenerated each day in order to maintain normal vision.

At the cellular level, RP is the result of the death of rod cells, followed by the death of cone cells. (Some forms of the disease begin with degeneration of the cones instead of the rods, but this is less common.) In fact, peripheral vision loss is usually the first noticeable symptom of the disease because the rod-to-cone ratio is highest in the periphery and so death of these rods leads to the sensation of tunnel vision. Cone death eventually follows rod death, and results in further (and more noticeable) loss of vision. It is not completely clear if cones die as a result of an inhospitable environment created by dying rods (i.e. cellular debris, reactive oxygen species (ROS), loss of vasculature to support them, etc.) or if they die as a direct result of a lack of a factor secreted by the rods themselves. For some time, such a factor was hypothesized, but not identified, but in 2009, Yang et al. reported in the journal *Molecular Therapy* the presence of rdCVF, that is, rod-derived cone viability factor, the lack of which could be the reason that cone death follows rod death (Elachouri, 2015).

Mechanism of Photoreceptor Cell Death in RP

Phenotypically, there is still some debate over whether cells in the RP retina die via necrosis, also known as catastrophic cell death, or apoptosis, a more controlled, programmed form of “cell suicide”.

In 2007, Marigo reported in a review that all investigated forms of RP indicated death via apoptosis, but the mechanism of apoptosis in each type of RP remains disputed. Whether it results in apoptosis or necrosis, it is widely held that photoreceptors in RP die due to ER stress and that the unfolded protein response (UPR) pathway which is activated when mutations in the gene produce a misfolding protein, plays a role (Rana, 2014 & Wang, 2014).

Rhodopsin’s Role in Vision: A closer look

Rhodopsin is a G-protein coupled receptor (GPCR) found exclusively in rod cells, and is sensitive to light. Technically, it consists of two main components: rod opsin and 11-*cis*-retinal. The opsin protein is a 7-transmembrane receptor with 3 regions, the C-terminal cytoplasmic region, the transmembrane region and the N-terminal intra-discal region which is located between the membranous discs of the rod outer segment. 11-*cis*-retinal is a small chromophore molecule that is covalently bonded to the rod opsin and switches from a *cis* to an *all-trans* conformation when exposed to light. When retinal isomerizes due to light it induces a conformational change in opsin as well, allowing it to interact with the G-protein transducin and setting off a cyclic guanosine monophosphate (cGMP) cascade, that eventually culminates in depolarization of the cell and a firing of

the rod neuron. (See Figure 4.) The role of rhodopsin in light/dark vision is essential and without it rods would be insensitive to light. Even minor mutations can cause reduced rhodopsin functionality, or can cause the aggregation of misfolded rhodopsin proteins, stressing the cell sometimes even to the point of death.

Early on, by sequencing the *RHO* gene of RP patients, scientists noticed that *Rhodopsin* mutations were often associated with autosomal dominant RP (adRP). However, studying the mechanism whereby each mutation causes rod death can be tricky. The effect of these RHO proteins on a cell are difficult to study *in vivo*, and progress of disease is relatively slow. Instead, the mutations have been studied *in vitro* in order to understand more fully their effect on cells, and the work presented here represents another iteration of the effort to characterize genetic variants in an efficient and meaningful manner. The earliest strategy to study *RHO* variants was developed by the Nathans' lab in 1991. They used a transfection system based on the human embryonic kidney cell line 293S and developed an enduring classification system based on protein production and accumulation in the cell, absorbance spectrum, the ability to regenerate with 11-cis-retinal, and protein localization to the plasma membrane. Briefly, their classification for *Rhodopsin* variations consisted of two main classes: Class I referring to those mutants which were similar to wildtype in regard to amount produced and which resulted in a low level of aggregation, and Class II mutants which were found at lower levels in the cells compared to WT and which were not properly localized to the plasma membrane. They further differentiated between Class IIa mutants, which fail to exit the ER, and Class IIb, which accumulate in both the ER and the plasma membrane (Sung, 1991 & Sung, 1993).

Three years later, the Khorana lab developed a similar system to test newly discovered variants using the African green monkey kidney cell line Cos1 to characterize 50 *RHO* variants (adding to the original 13 published by Sung et al.) (Kaushal, 1994). Using protein localization, spectra absorbance, ability to bind to and activate transducing and chromophore regeneration, they defined three classes of *RHO* mutants, which were similar in many respects to the classes set out by Nathans. Synthesizing the studies that had come out over the previous decade, Mendes et al. proposed a new classification system based on 120 naturally-occurring rhodopsin mutants and broke them down into six nuanced categories in their 2005 publication (see Fig. 5).

A decade later, using HEK293 cells, McKeone et al. developed yet a new way to to characterize the growing number of discovered *RHO* variants (McKeone, 2014). Their assay, which featured a GFP-tagged Rhodopsin, incorporated FACS technology to correlate computer predictions of folding instability to severity of the RP phenotype in patients. Building upon the protocol developed by McKeone et al., our experiments utilize HEK293 cells and FACS in a protein localization assay that identifies potentially pathogenic genetic variants.

But *how* do the phenotypes outlined in the classification scheme result in cell death? Usually, when proteins like Class II mutants misfold or are not translocated to the correct target location they form aggregates in the endoplasmic reticulum. This build-up of misfolded proteins causes activation of the so-called “Unfolded Protein Response” or UPR, also known as the ER-stress cascade. In fact, studies on the P23H mutant form of rhodopsin have shown conclusively that it does induce ER stress, leading to cell death, and is exacerbated by light exposure, due to the effect of light on this form of the protein

(Tam, 2014). (NB: Light exposure does not matter in the experiments described in the work presented here, since the rhodopsin is not bound to a retinal chromophore.)

When a protein is folded incorrectly, the cell will down-regulate its translation as part of the UPR as well as begin to synthesize more chaperone proteins to help correct the folding. If that doesn't work, then the incorrectly folded proteins are moved from the ER to the cytoplasm where they are tagged with ubiquitin, which targets them for destruction within the proteasome. However, wildtype rhodopsin is produced at such great quantities (5×10^7 molecules/rod/day) within rod cells that when faulty rhodopsin is created, it is created *en masse* and soon overwhelms the cell. When the UPR is not able to keep up with the amount of protein that it needs to dispose of, the misfolded proteins may form aggregates, and eventually the UPR, instead of being geared towards fixing misfolded proteins, will tend towards inducing apoptosis.

Disease Model Systems

When researching a disease, it is ideal to work in a context that is as faithful to the *in vivo* situation as possible, while also as cost effective as possible. On one end of the spectrum are *in vivo* models, which are expensive and time consuming, though which obviously afford the best observation of cells in their native environment. The mammals which are most often used for retina research are monkeys, rabbits, cats and mice. Of these, mice are the most cost effective. Unfortunately mouse and human retinas differ in ways that are not insignificant, the most striking of which is that the mouse retina does not have a fovea. On the other end of the spectrum, *in vitro* models are more cost

effective, but do not recapitulate the microenvironment of a cell within a living system. On the other end of the spectrum, transfection of genes into non-retinal cell lines represents a very common *in vitro* method to study the effects of gene expression. Beyond that, there are cell lines derived from retina that are available for purchase. However, again, in cell culture, the *in vitro* environment is a far cry from the specialized cellular microenvironment where a photoreceptor is naturally found.

Recently, a new model system for retina research has been developed that has the convenience of an *in vitro* system, but some of the specialized microenvironment of an *in vivo* system. A few different versions of such a system have been developed. One, published in 2011 in *Stem Cell*, relies on differentiating human induced pluripotent stem cells (hiPSCs). By adding growth factors to differentiate the cells into an ectoderm lineage, Meyer et al. showed that it was possible to develop retinal and forebrain cells, and that separation of developing retinal cells from developing forebrain cells was possible. This represented the first hopes for personalized medicine for retinal diseases (Meyer, 2011). Two years later, a similar system was established using mouse embryonic stem cells (mESCs). The system is based on culturing mESCs in a biological matrix until they produce whole embryoid bodies (wEBs) (Gonzalez-Cordero, 2013). When specific protocols are followed, the embryoid bodies begin to invaginate and produce first optic vesicles, and then optic cups. The cells in these induced optic cups have been shown to produce markers for photoreceptor lineage and so have been deemed photoreceptor precursor cells. They have also been successfully transplanted and integrated into host mouse retina (though integration rates remain low and functionality questionable).

Clearly this will be an exciting field to monitor in coming years as the techniques are refined.

Current State of RP Therapy

Currently, there is no cure for RP, and patients that present with a confirmed case are fated to progressively lose vision for the remainder of their lives. There are some purported methods for slowing progression, such the administration of neurotrophins and anti-apoptotic factors, but though they have shown promise for preserving retinal architecture, there is less evidence that it has helped sustain photoreceptor function (Liang, 2001 & Berger, 2015). Some doctors also recommend wearing light-filtering lenses to block more harmful forms of light and thus slow progression, but this is not a common prescription (Parmeggiani, 2011). Among these therapies, all are palliative and none truly have been shown to stop, or even significantly slow progression. However, there is much hope for gene therapy for RP patients, where there has already been some success.

Since, anatomically speaking, the eye is an outgrowth of the brain, with tight junctions between RPE cells forming a barrier between the eye and the circulatory system, it basically forms an extension of the blood-brain-barrier known as the blood-retina-barrier (BRB). Because this creates an immunologically privileged space, gene therapy delivered to the eye is less dangerous than when administered systemically, since the delivered gene is hypothesized to stay within the confines of the eye and not spread to other parts of the body. Indeed, some success with gene therapy on retinal degenerations

include delivery of a corrected *RPE65* gene to patients with Leber congenital amaurosis (LCA) with dramatic, vision-saving results early-on in gene therapy exploration (Bainbridge, 2008, Maguire, 2008 & Hauswirth, 2008). More recently, there have been promising results with gene therapy involving the *REPI* gene for choroideremia (MacLaren, 2014). Gene therapy has been tested in the mouse as well, with a corrected form of *RHO* being delivered to *RHO-P23H* mice via AAV and resulting in successful rescue (Mao, 2012). In addition, gene editing technology using Crispr/Cas and iPS cells may comprise the future of gene therapy for RP patients (Zheng, 2015).

Significance

Retinitis pigmentosa is a fairly common disease, but one which is complicated by having hundreds of actual and potential genetic causes. If a method could be developed that could test several candidate genetic variants at once, it would be a great boon to the field of research for this disease. The following experiments describe a newly developed system to efficiently and relatively easily characterize potentially pathogenic variants of unknown significance (VUS) discovered through NGS sequencing of patient DNA. The system consists of three main parts: 1) a flexible plasmid vector used to deliver various versions of the target gene to cells in culture via transient lipid transfection, 2) a FACS-based protein localization assay and sorting, and 3) NGS sequencing. It is hoped that the flexibility of the described system could be used beyond the application for *RHO* variants described here.

Chapter II

Materials and Methods

Creation of Library

Preparing plasmid vector backbone for use in the Gateway Cloning system: A plasmid carrying the Gateway Reading Cassette (GWRC) (Life Technologies) and a vector backbone were restriction digested with EcoRV. After incubation with calf intestinal alkaline phosphatase (CIAP) (to prevent self-ligation) they were then ligated to each other using T4 DNA ligase (Life Technologies). The resulting plasmid consisted of a chicken actin enhancer (cag), a V5 tag, the inserted cassette, an internal ribosome entry site (IRES) followed by the fluorophore mCherry (mCh) (Addgene), a pBR322 origin of replication (ORI), and an ampicillin resistance gene. The final plasmid backbone, dubbed pcag-V5-GW-IRES-mCh for short, was Sanger sequenced at each step to assure faithfulness to the original sequences and proper orientation of the ligated pieces. Plasmids were propagated in ccdB survival cells (Life Technologies) and integration of all parts of the vector and gateway reading system was confirmed via chloramphenicol dependence and ampicillin resistance.

Preparing plasmid insert for the use in the Gateway Cloning system: A pDONR *Rhodopsin* plasmid was purchased from GeneCopoeia (GC-T1321). The *Rhodopsin* gene was then mutated via site-directed mutagenesis using a one-primer modification to the

QuikChange II protocol from Agilent (Braman, 1996). RP-associated variants reported in the literature as well as variants of unknown significance (VUS) found in patients at MEE (unpublished) were created. Using codon usage charts, synonymous mutations at the 3' end of the *RHO* gene were also created to act as transfection controls in future experiments and to ensure that the mutagenesis reaction itself did not induce a phenotype when the transfected genes were expressed. The wildtype (WT) synonymous mutations were designed on the 3' end of the gene in order to minimize any possible (though unexpected) changes to transcriptional or translational processes (Stoletzki, 2007). Plasmids were propagated in One Shot Top10 chemically competent E.coli (Invitrogen) (or similar) and successful integration of the insert into the plasmid was confirmed via antibiotic resistance to kanamycin.

After preparation and Sanger sequencing of the plasmid backbone and inserts of *RHO* variants, the backbones and *RHO* inserts were joined using LR Clonase II technology (Invitrogen) which joins gateway compatible plasmids using a proprietary enzyme mix that relies on unique properties of recombination in the bacteriophage lambda (Landy, 1989). The resulting expression clone consisted of: pcag-V5-*RHO*(WT or variant)-IRES-mCh and was propagated in Stbl3 cells (Invitrogen) and successful integration of the two pieces was confirmed via ampicillin resistance. Plasmid DNA was collected and purified using miniprep technology (Qiagen) (or similar) and the DNA subjected to analytical restriction digests and Sanger sequencing to confirm correct nucleotide sequence.

Mammalian Cell Culture

Cos7 and HEK293 cells (ATCC) were cultured using aseptic technique and grown in 10% fetal bovine serum (FBS) in Dulbecco's Modified Eagle Serum (DMEM) without antibiotics. Cells were grown at 37°C and 5% CO₂ in a standard cell culture incubator. Cells were passaged at subconfluent densities every 2-3 days as needed.

Transfection for Microscope Viewing and Rating

Transfections were performed using Lipofectamine 2000 (Invitrogen) on coverslips in 6-well tissue-culture plates (BD). Briefly, uncoated glass coverslips with a 25mm diameter were placed in wells and Cos7 cells seeded on top at a density of 200 cells/mm² in 2mL fresh media. The next day, 2ug plasmid DNA and 3uL Lipofectamine in 150uL Optimum reduced serum media (Gibco) were used for the transfection. Cells were returned to the incubator for 48 hr preceding collection.

Immunocytochemistry for Microscope Viewing and Rating

To stain transfected Cos7 cells on coverslips, wells were first washed briefly with phosphate buffered saline (PBS), and then fixed in 1mL 4% PFA for 20 min and then washed twice in PBS for 5 minutes. Cells were blocked with 1% BSA in PBS applied for 5min and then Rhodopsin antibody, epitope Ret-P1 (Sigma) was applied at a final concentration of 1:200 in blocking buffer for 1 hr. After washing with PBS, Alexafluor-488 goat anti-mouse antibody was applied in blocking buffer at a final concentration of

1:1k for 1 hour. Cells were left in PBS O/N. Before coverslipping, cells were washed in PBS with Hoechst stain (Life technologies) applied for 1-5min at a concentration of 1:5k. Coverslips were drip-dried and mounted cell-side down onto slides containing ~50uL Fluoromount G and dried overnight. Slides were viewed at 200x using a Nikon TI Eclipse microscope and rated on a scale of 1-4 based on their Ret-P1 staining. Scores were based upon the comparison of each variant to WT (normal expression=3) and Rho P23H (low expression=1). Using these standards and blinded to the identity of the transfected variant being viewed, the slides were viewed and rated by the same scientist on 3 separate occasions. Each variant was then assigned a final score based on the average of these three scores.

Transfection for FACS

Transfections were performed using Lipofectamine 2000 (Invitrogen) in 24-well plates as described previously (McKeone, 2014). Briefly, HEK293 cells were seeded at a density of 200 cells/mm² in 24-well tissue culture plates. The next day, the media was changed and cells transfected with 0.5ug plasmid and 1.5uL Lipofectamine in 50uL Optimem. Cells were returned to the incubator for 48 hr until collection for FACS staining.

Flow Cytometry

On collection day, wells were first washed briefly with PBS. 200uL trypsin was added to each well and allowed to incubate for 4 minutes at 37°C. 300uL full media was then added, the media was triturated to dislodge all cells from the bottom of the dish, and cells collected into 2.2mL tubes. Tubes were centrifuged at 400 xg in a floor centrifuge for 4 min. Cells were washed one time with 500uL PBS and then resuspended in 4% PFA in PBS or non-diluted zinc based fixative (ZBF) (Sigma) for 20min in the dark. After fixation, cells were washed once in 500uL PBS and then resuspended in 250uL 3% BSA in PBS and 250uL of antibody added. Anti-Ret-P1 antibody was used at a final concentration of 1:1k, with an incubation time of 30 minutes. Secondary antibody was used at a final concentration of 1:300 and also incubated for 30 minutes. Cells were then washed once more in PBS and resuspended in 300-500uL PBS for use with the LSRII flow cytometer (BD) at the MGH Pathology Core facility. For sorting, gates were set using WT and P23H single populations and then a mixed population of cells was sorted into PBS containing 1% FBS. Results were analyzed with Flowing Software (<http://www.flowingsoftware.com>). Percent of cells with high RHO surface expression was determined by setting the quadrants based on the WT and P23H controls in each experiment and then dividing the percent of cells in the top right quadrant (double-positives) by the sum of the top right and bottom right quadrants (double positives plus single positives). The transfection was done 3 separate times, twice in duplicate, and the results averaged.

RHO Plasmid Extraction from Sorted Cells

Sorted cells were spun down, supernatant removed and then resuspended in Buffer P1 in preparation for use with the plasmid miniprep protocol (Qiagen). Plasmid DNA was eluted in 35uL Buffer EB for use in PCR amplification.

RHO PCR Amplification

PCR Amplification was performed on the plasmid DNA extracted from FACS sorted cells using forward primer: GTTTGTACAAAAAAGCAGG and reverse primer GGAATTTACGTAGCGGC which were complementary to regions of the plasmid DNA on either side of the *Rhodopsin* sequence. HotStarTaq (Qiagen) polymerase was used with the following PCR program: 1) 95°C for 15min; 2) 30 cycles of: 94°C for 30sec, 50°C for 30sec, 72°C for 1min; 3) 72°C for 10min as final extension. 1uL of the result was then run on a Tapestation (Agilent) to determine appoximat size and concentration and to confirm presence of a single band. PCR reactions were cleaned up via Qiagen PCR clean-up kit and then submitted to the MGH CCIB Core for complete plasmid sequencing. Complete plasmid sequencing data was analyzed using a custom-written software program developed by Dr. Jason Comander at MEE.

Chapter III

Results

For genetically heterogeneous diseases such as RP, discerning whether new genetic variations are benign or deleterious is key to effective diagnostics and for future therapies. Here, we outline a protein localization assay with which to test genetic variants newly discovered via NGS in order to make an informed prediction about their pathogenicity. Using the transfection-based model of McKeone et al. as a springboard for our own method, we have created a flexible assay with the added ability to characterize several variants simultaneously by combining FACS and NGS.

A plasmid with the human *Rhodopsin* sequence was cloned into a gateway compatible vector and variants made using a modified one-primer method of site-directed mutagenesis (Braman, 1996). This library of *Rhodopsin* variants were then individually inserted into a vector backbone via Gateway technology using LR Clonase. Each final expression plasmid in the library contained a chicken actin promoter with CMV enhancer (pcag), V5 tag, *Rhodopsin* gene, and an internal ribosome entry site (IRES) which drove the expression of the fluorescent marker mCherry, which was used as a marker for successful transfection (Fig. 6). See Table 1 for a list of mutants that were used for these pilot experiments.

We first transfected variants into Cos7 cells. Cos7 green monkey kidney cells were chosen because of their large size, which allows for easy visualization of protein localization after staining. It is also closely related to the type of cell (Cos1) in which the Nathans lab did their groundbreaking research when first studying mutant rhodopsin localization in the cell (Nathans, 1994). After 48 hours, cells fluoresced in the mCherry channel, indicating successful transfection. We then stained for surface localization of Rhodopsin with Rhodopsin Ret-P1 primary antibody, which labels the N-terminus of the protein (Fig. 7). For FACS, HEK293 cells were transfected and stained in a similar fashion to the Cos7 cells and run on an LSRII flow cytometer (BD) for analysis. Despite the difference in cell type, the intensity of the fluorescence read by the FACS machine correlated positively with the immunofluorescence ratings assigned to the transfected Cos7 cells (Fig. 8, Fig. 9). Confident that our fluorescence assay was working, we continued to pursue the FACS assay as an efficient and quantitative method of analysis.

Following the protocol of McKeone et al, HEK293 cells were made to take up plasmid via lipid transfection (see Materials and Methods for more details). 48 hours after transfection, cells were stained with Ret-P1 RHO antibody to allow for detection of RHO-surface expression. Cells that had been transfected with known Class II mutant P23H, which produces a mutant protein that is known to localize to the endoplasmic reticulum and not effectively reach the cell surface was easily distinguishable from WT both by immunofluorescence (Cos7 cells) and by FACS (HEK293 cells) (Fig 8). To determine the percentage of transfected cells with high surface RHO expression, we applied quadrants to the FACS plots (Fig 8, D-F). To control for inter-experimental differences while applying a fair standard to all samples, new quadrants were drawn for

each experiment, based on the plots of WT and P23H. The same quadrants were then applied to every sample plot within one experiment and data generated from these plots using Flowing Software. When plotting mCherry expression (transfection marker) on the X-axis of a FACS dot plot and Alexafluor-488 on the Y-axis (RHO surface expression), we considered everything on the right side of the drawn quadrants to be transfected cells, which had a high level of mCherry and thus plasmid expression. To determine the percentage of transfected cells with high surface RHO, the percentage of cells in the top right quadrant was divided by the sum of the percentage of cells in the top right and the bottom right quadrants. Using this formula, 92.97% of cells transfected with *RHO-WT* exhibited high RHO surface localization, compared with 12.45% of cells transfected with *RHO-P23H* (average of samples from 3 separate transfection experiments). Running a two sample two-tailed t-test reveals a significant difference with $p < .001$. Transfection with plasmids that contained “silent” WT synonymous mutations were indistinguishable from WT, showing on average 93.72% transfected cells with high surface RHO ($p > .05$) and therefore not a significant difference from WT. Non-transfected cells showed virtually no background, with neither mCherry nor secondary antibody Alexafluor-488 detectable in either right-hand quadrant via FACS (Fig 10).

We tested eight *RHO* VUS from a cohort of RP patients at MEEI and four *RHO* plasmids with WT-synonymous (ie. genetically silent) mutations. Our assay revealed one potential Class II mutant (Variant 203), with a phenotype similar to P23H, showing 11.46% of transfected cells with high surface RHO ($p < .001$). Variant 197 exhibited an intermediate phenotype: 61.04% of transfected cells had high surface RHO ($p < .001$). The other VUS tested yielded phenotypes similar to WT; though Variant 198 and Variant 200

had a slightly lower average percentage of transfected cells with high surface RHO, 88.38% and 88.94% respectively, it was still one-and-one-half-fold higher than Variant 197 and about seven-fold higher than P23H or Variant 203. See Figure 10 for a full summary of results.

We then predicted that if mixed, we could successfully sort transfected (ie. mCherry-positive) cells into two populations of high and low surface RHO expressers and then interrogate the plasmid DNA in the two groups post-sort. To test this strategy, we first did a pilot FACS analysis with only *RHO-WT* and *RHO-P23H* plasmids. Looking at an overlay of the dot plots from the FACS analysis revealed a bimodal shape (Fig. 11). Sorting a mixture of the WT and P23H cells on the sorter was successful in that P23H plasmid was found in greater abundance in the “Low” population and WT found in greater abundance in the “Hi” population (data not shown).

We next FACS sorted a mixture of cells that included cells from wells individually transfected with the 8 VUS, 4 WT synonymous variants and *RHO-P23H* (eg. Variant 6, which served as a positive control). By setting gates based on *RHO-WT* and *RHO-P23H*, we sorted the mixture into two populations of transfected cells (ie. high mCherry): those with high RHO surface expression (ie. high Alexafluor-488, dubbed “Hi”), and those with low RHO surface expression (ie. low Alexafluor-488, dubbed “Lo”). In order to maintain the integrity of the DNA of the cells without fixative-induced cross-linkages like those caused by paraformaldehyde, these cells were fixed with zinc-based fixative (Sigma). 24,065 cells were sorted into the Hi group and 4,251 cells were sorted into the Lo group.

To determine the *RHO* variants present in each sort group, plasmid DNA was extracted from the cells using a plasmid miniprep kit (Qiagen). We then used PCR to amplify the *RHO* portion of the plasmids and the resulting linear sequences were sent for NGS analysis to discern which variants were present in each pool. Using a custom-written software program to interpret the results of the NGS analysis, it could be determined how many reads of each variant was found in either the Hi or Lo group and the ratio between them calculated (data not shown). If the ratio of Hi to Lo was greater than 1, the variant was more often found in the Hi population and thus produced a high surface RHO phenotype; if the ratio was less than 1, the variant was more often found in the population with a low surface RHO phenotype. Using this approach, *RHO-P23H* has a ratio of 0.27, while WT synonymous Variant 207 has a ratio of 2.19. The results of the NGS analysis correlated positively with the results of the standard FACS analysis described earlier, though the results from Variant197 and Variant195 do not correlate as well as the other samples. See Figure 12 for a comparison between the two methods of analysis. Table 2 contains a summary of all results along with predictions of pathogenicity based on these results.

Chapter IV

Discussion

The wealth of data produced by NGS methods can be difficult to wade through and, when it reveals variants of unknown significance (VUS) it can mean frustratingly ambiguous results for patients and genetic counselors alike. Most current methods rely on *in silico* (ie. computer modeling) predictions of pathogenicity of VUS, or else testing of VUS one-by-one, which is extremely time-consuming and delivers results outside the context of related variants. Here we report a method whereby several VUS can be tested simultaneously for a mislocalization phenotype that belies Rhodopsin-related pathogenicity. By utilizing a transfection plasmid system, VUS (in this case, in the *Rhodopsin* gene) can be expressed in cultured cells, the localization of Rhodopsin determined by FACS, the transfected cells sorted by phenotype and the plasmids in each group identified. An efficient test of VUS protein localization phenotype has thus been developed, and the flexibility of the system leads us to hope that this system could be applied to other genes, diseases and assays in the future.

The immunocytochemistry experiments build upon the protocol performed by McKeone et. al which used a GFP-tagged Rhodopsin in a FACS assay. One key difference in the system described here is the use of an IRES-mCherry construct instead of a Rhodopsin-GFP fusion protein as a transfection marker. This can be viewed as an improvement, since the protein produced by the expression plasmid is more likely to act

like wildtype Rhodopsin when it is not encumbered by extra transgenic peptides; it is more likely to be trafficked as an endogenous protein than a fusion protein would be. In addition, the possibility exists to switch out the mCherry fluorescent marker with any number of other fluorescence genes (eg. cerulean, dsred, GFP) with a relatively simple ligation procedure, thus giving our system a flexibility not easily achieved with fusion proteins.

Indeed, flexibility is one of the strengths of the system described here since various parts of the expression plasmid (eg. promoter, tag, target gene, IRES, fluorescence gene) have the potential to be switched out for alternative sequences for ease of use or to use in conjunction with other assays. Although a library of *Rhodopsin* mutants was used here, it is the hope that the same method could be used on other, similarly-sized genes by creating a pDONR library through site-directed mutagenesis and utilizing LR clonase to create expression clones in the manner described here. Furthermore, though this assay focuses on protein localization (intracellular versus surface) as the main readout, using this type of expression plasmid could perhaps be harnessed for use in other assays or readouts, depending upon the function or localization of the translated protein. Moving from plasmid to virus is also a possibility, using the building blocks of the plasmid system described here, for use *in vitro* or even *in vivo*.

One obstacle to be overcome in the development of this system was to identify a staining method that would suit the needs of the protein localization assay. By staining with a primary antibody that detects an epitope on the N-terminus of the Rhodopsin protein (clone Ret-P1) and by refraining from permeabilizing the cell with detergent during the staining procedure, we were able to detect solely surface expression of

Rhodopsin. (See Figure 13 to see the effect of permeabilization with TritonX-100 on the staining procedure.)

The system described here is limited in its ability to categorically predict VUS pathogenicity in that it can only positively identify Class II mutants that cause cell death via overloading the ER with misfolding proteins. However, Rhodopsin mutants of other classes, which are also implicated in rod death in RP, act by a different mechanism of cell death. An area of ongoing research is to modify the protein mislocalization assay described here in such a way as to be able to assay the affect of the variant on cell death. Using such a dual-pronged approach to assay both protein localization and cell death would be an efficient method of screening many VUS simultaneously and lend even greater confidence to the resulting predictions of pathogenicity. However, it may prove difficult to develop a cell death assay based on transient transfection, since RP is a slow-acting disease and the cell death seen in RP may not easily be recapitulated *in vitro*.

One strength of this assay is found in the ability to FACS sort a pool of variants by phenotype and recover the DNA afterwards. It is this aspect of the assay that gives it the power to test many variants simultaneously, and which may drastically cut the time needed to individually assess each variant. In addition, as more and more variants are added, it raises the possibility that new patterns may emerge. Since there is already a wealth of data available about most of the (published) RHO variants in the library, as their FACS plots and sort ratios are studied, it could be seen that certain classes of mutants (other than Class II) group together or create some other sort of pattern that is yet undetectable. Another possibility is that in the context of many other variants, the

character of VUS with an intermediate phenotype may be elucidated as when compared to known mutants that have a similar phenotype.

It was a major challenge to figure out how to isolate plasmid DNA from a small number of FACS-sorted cells. Although fixation with paraformaldehyde (PFA) gives the clearest FACS plots and separation of high-surface expression vs. low-surface expression populations, the cross-linking properties of PFA make it problematic for post-experimental DNA isolation. Instead, a zinc-based fixative was used for the cells that would be sorted. Though the separation of populations is not as clear as for PFA-fixed cells (see Fig. 13), the damage to the DNA is much less, and allows for the successful isolation of plasmid DNA from the sorted cells.

The amount of DNA isolated from these tens of thousands of fixed and sorted cells was obviously very small. Therefore, PCR amplification was necessary to enable the discovery of which plasmids segregated to a population with a wildtype-like phenotype versus a mutant-like phenotype. In the method described here, there is no way to tell whether *RHO* that is being amplified is from a plasmid within the cell or from plasmid stuck to the outside of the cell membrane. In the future, it would be advisable to use a reagent such as CellScrub which can rid cells of extracellular plasmid that may be adhered to the outside of the cell but not actively transcribed or translated, so as to lend more credibility to the results of the PCR. Another way to increase the faithfulness of the assay is to extract RNA from the sorted cells instead of plasmid DNA. In this method, DNase would be applied to the RNA during the course of extraction, thus eliminating the possibility of *RHO* amplification from extracellular plasmid. An RT-PCR reaction would need to be performed, which creates cDNA from the isolated RNA and then amplifies it

during PCR. This is preferable to the method described here since the region that is amplified by PCR is being actively transcribed or translated in the cell. We attempted this process once but were not able to amplify a sufficient amount of cDNA for NGS analysis. We plan to attempt this again in future experiments and increase the cycles of the PCR in hopes of boosting the signal.

Another planned improvement for this experiment is to explore the possibility of decreasing the number of individual transfections before sorting. If one transfection could be done using multiple plasmids, and the same results obtained as doing multiple individual transfections and then mixing the cells (as described here) this would even further reduce the time and reagents needed to test several VUS at once, which is the overarching goal of the project. One challenge to this method is ensuring that every plasmid be successfully transfected into the cells, which is difficult since the WT plasmid may be preferentially transcribed and translated. At this point, separate transfections is necessary, but hopefully this need will be overcome in the future with new methods.

One drawback to our system is that it can only necessarily help to discover dominant mutations, and will reveal nothing about recessive mutations. However, since mutations in *RHO* account for up to 40% of autosomal dominant RP and new *RHO* mutations are still being discovered, or have an unknown effect, the motivation to identify dominant mutations is in fact very strong in the general public, and is by no means a fruitless study.

In conclusion, we report here a new *in vitro* method to predict potential dominant Class II pathogenicity of *Rhodopsin* VUS via two complementary methods. We first

describe a method of FACS analysis that groups VUS into categories based on RHO surface expression. We next present a method by to group variants by FACS sorting a mixture of transfected cells and then interrogating the plasmid DNA taken up by them. The assay could be adapted for other genes and phenotypes, as long as they can be distinguished using a two fluorophore system: one that is built into the plasmid as a transfection marker and one that is used as a phenotype readout, such as the RHO antibody detection described here. Our work serves as proof of concept that we are able to efficiently pool and then deconvolute a mixture of cells transfected with similar genetic variants. This assay serves as a new tool in the effort to efficiently interpretation the vast amounts of data discovered via NGS. As new potentially pathogenic variants are identified and tested in this way, research can be focused on the clearly deleterious ones and perhaps develop therapies to address them.

Appendix

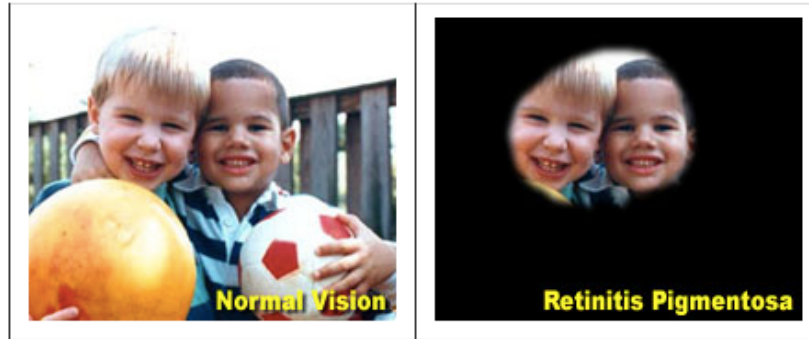


Figure 1. Normal versus RP vision. The figure on the right represents a simulation of the vision experienced by a patient with Stage II RP, wherein there is pronounced tunnel vision due to peripheral rod death in the retina.

(Image courtesy of https://nei.nih.gov/health/pigmentosa/pigmentosa_facts.)

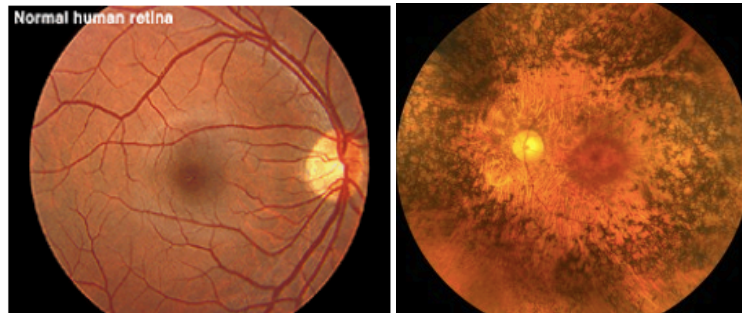


Figure 2: Normal versus RP fundus. Fundus photos of a normal human retina on the left, and an RP retina on the right. Note the pigmentation in the periphery as well as the thinning of blood vessels.

(Image courtesy of <http://webvision.med.utah.edu/book/electrophysiology/the-electroretinogram-clinical-applications/>)

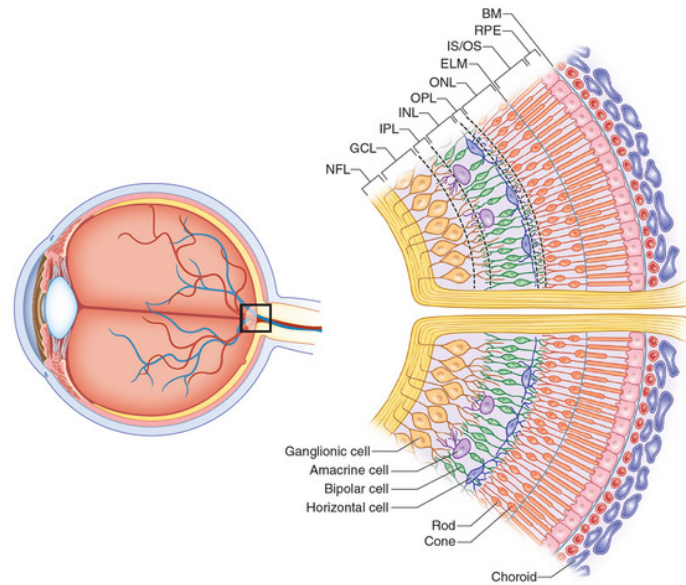


Figure 3: Schematic of eye anatomy. Rods and cones are located in the outermost layer of the retina and are supported by the retinal pigment epithelium (RPE). Note the difference in shape between rods and cones.

(Image taken from: <http://www.retinareference.com/anatomy/>)

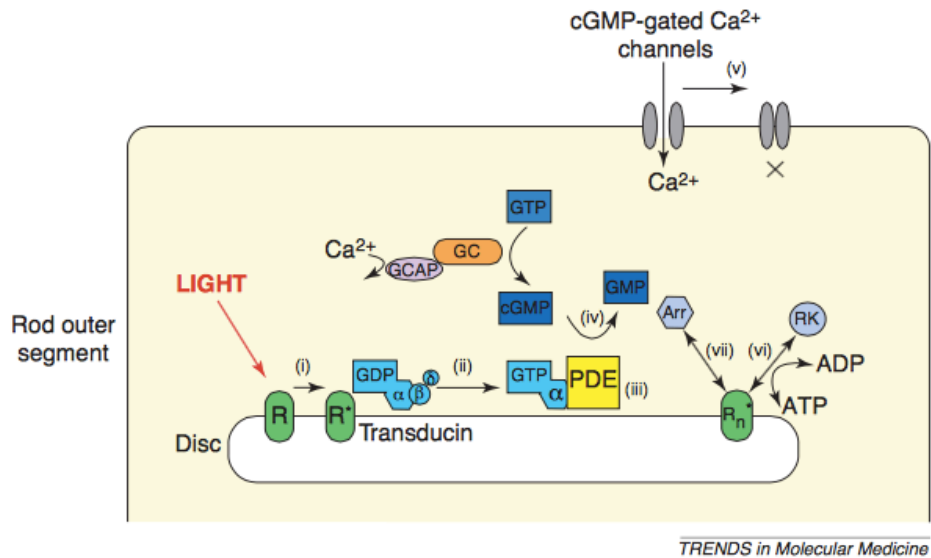


Figure 4: Light signaling cascade in rod outer segment. Rhodopsin (R) is termed R* when the 11-*cis*-retinal isomerizes to *all-trans*-retinal due to light and changes rhodopsin's overall conformation to allow interaction with transducin which eventually leads to a cGMP cascade.

(Figure from Mendes, 2005.)

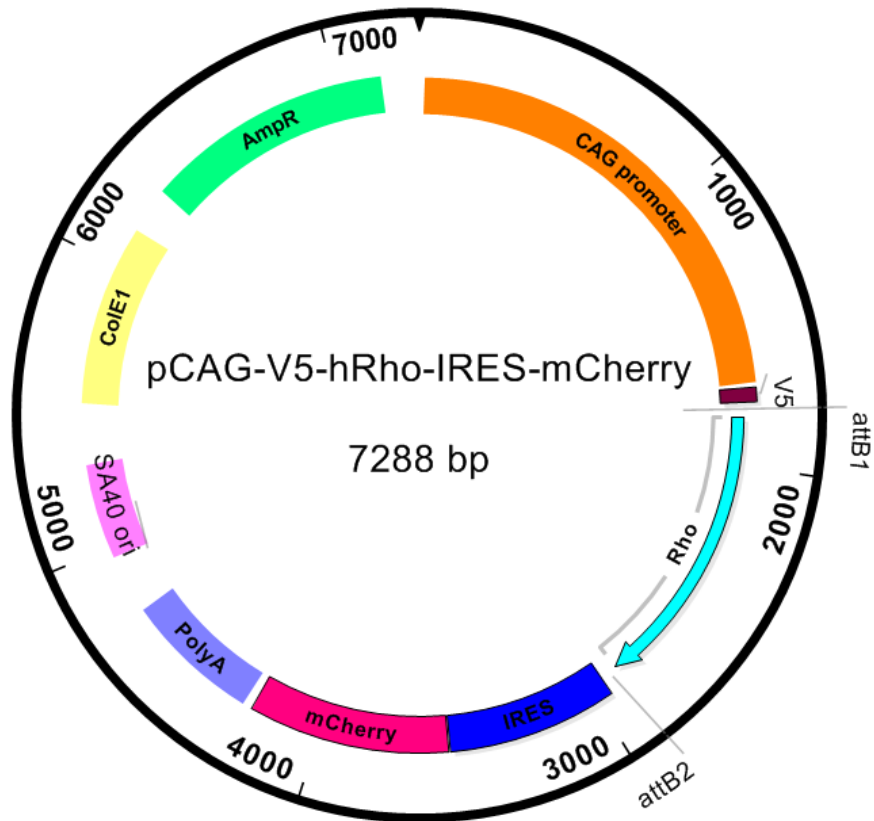


Figure 6: *RHO* expression plasmid used in transfections. *att* sites are found on either end of the region which is swapped during the LR Clonase reaction (Life Technologies). The entire plasmid is 7,288 base pairs (bp) long. The region coding for hRHO is 1047 bp.

(Map constructed using Lasergene SeqBuilder.)

Variant Number	Point Mutation	Amino Acid Change	Notes
6	c.68C>A	P23H	First reported: Dryja 1990
195	c.185C>A	T62N	VUS MEE
196	c.218A>G	N73S	VUS MEE
197	c.302G>T	G101V	VUS MEE
198	c.439C>T	R147C	VUS MEE
199	c.755G>A	R252H	VUS MEE
200	c.895G>A	A299T	VUS MEE
201	c.913A>G	I305V	VUS MEE
203	c.538C>A	P180T	VUS MEE
204	c.966C>T	none	Wildtype Synonymous
205	c.969C>T	none	Wildtype Synonymous
206	c.972C>A	none	Wildtype Synonymous
207	c.978C>T	none	Wildtype Synonymous
WT	None	None	Wildtype

Table 1. Rhodopsin variant table. Over 200 *Rhodopsin* variants were created via site-directed mutagenesis. The variant number is an arbitrary number assigned for ease of use and organization. For the experiments detailed here, Variant 6 was used as a control variant representing a Class II phenotype in which Rhodopsin is not translocated to the surface of the

cell. Wildtype synonymous variants have an engineered point mutation which differs from the WT but does not change the amino acid sequence. *VUS*: Variant of Unknown Significance. *MEE*: Massachusetts Eye and Ear.

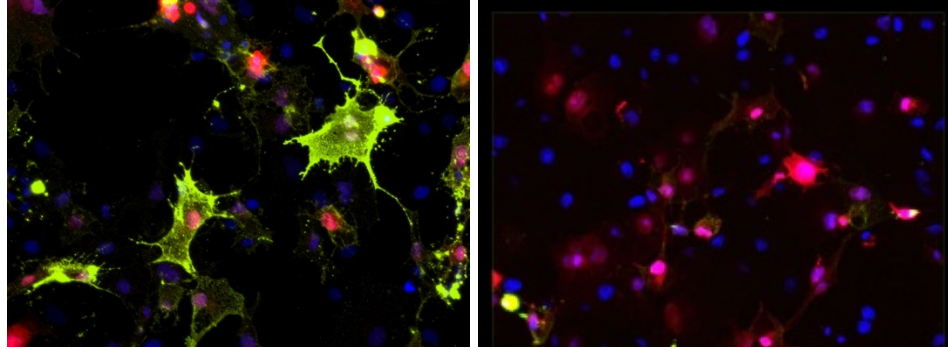


Figure 7: Rhodopsin surface expression in transfected cells. Merged fluorescent images of PFA-fixed Cos7 cells transfected with *Rhodopsin* expression plasmids and stained with Rhodopsin Ret-P1 primary antibody (Alexafluor-488, green). mCherry (red) fluorescence indicates transfected cells. Hoechst (blue) dyes cell nuclei. Left: Cells transfected with *RHO-WT*. Right: Cells transfected with *RHO-P23H* Class II mutant.

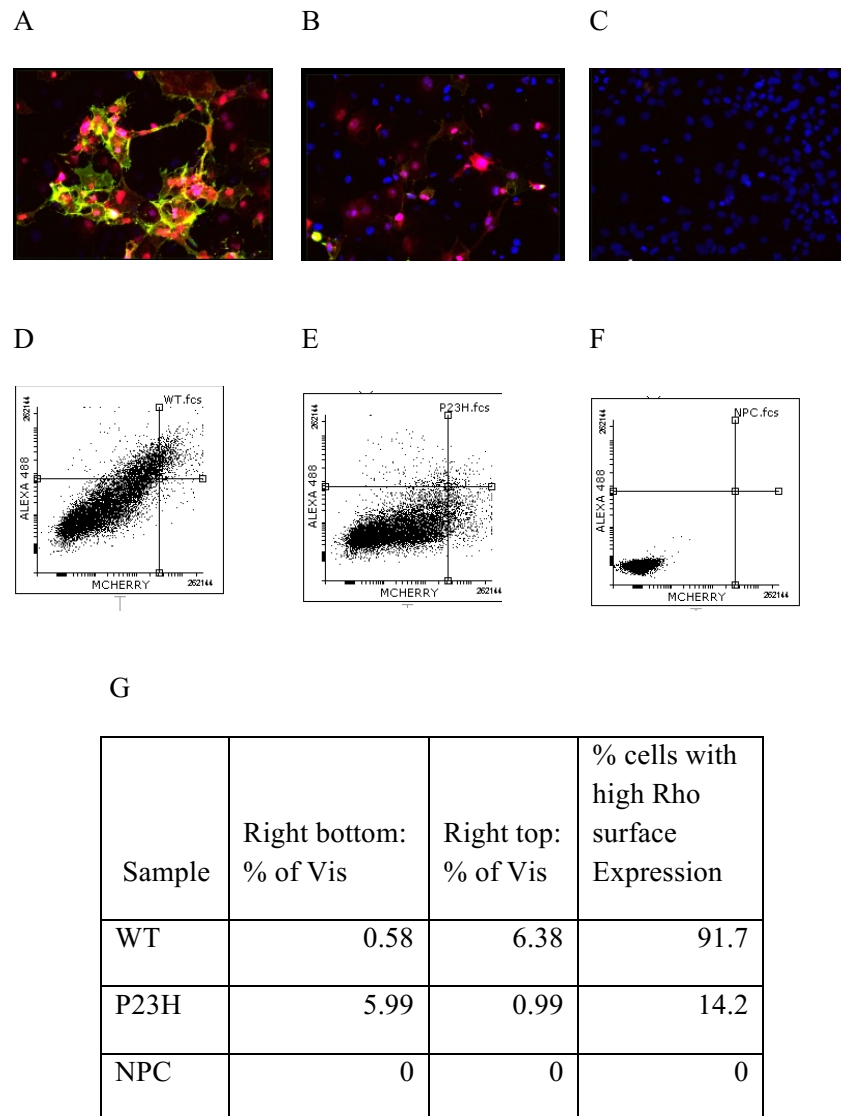


Figure 8. Immunocytochemistry compared to standard FACS assay. FACS plots correlate with immunocytochemistry, despite difference in cell type. Cos7 cells (A-C) or HEK293 (D-G) were transfected with *pcag-V5-hRho-IRES-mCherry* expression clones with the following versions of

Rhodopsin: Left column: *hRHO-WT*; Middle: *hRho-P23H*; Right: No plasmid control (NPC).

Cells were then stained for surface Rhodopsin (green, A-C). FACS readouts (D-F) correlate with the phenotype observed by eye under the microscope. Using Flowing Software, matching quadrants were added to the FACS plots and the percentage of transfected cells with high surface Rhodopsin was calculated (G).

Validating Surface Expression Assays

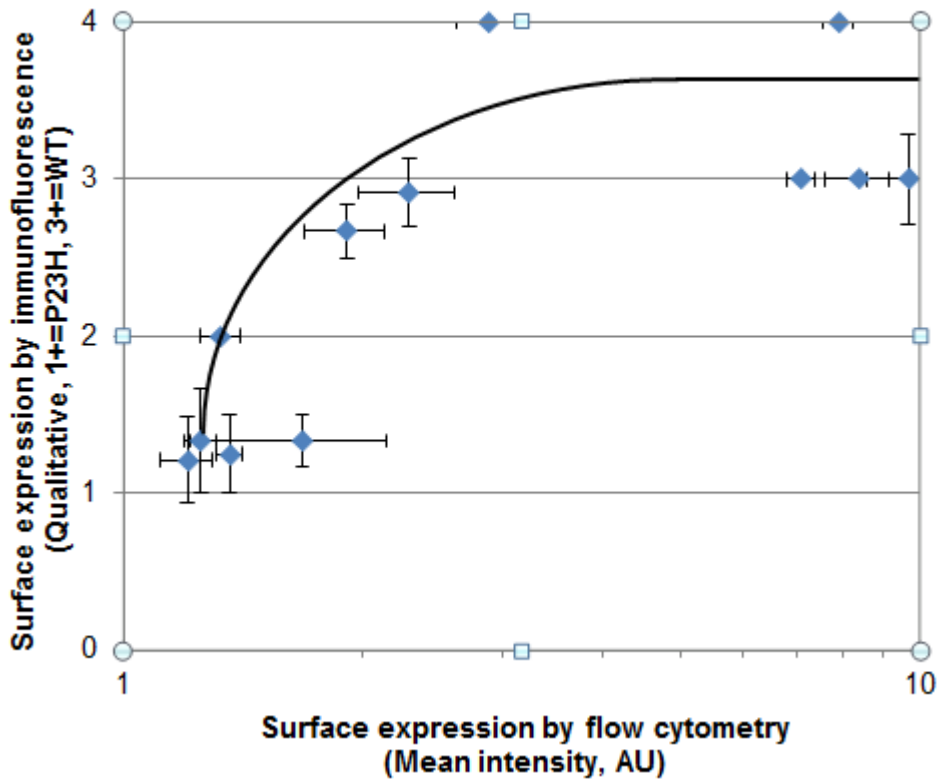


Figure 9: Validating surface expression assays. Transfected cells were stained with Ret-P1 Rhodopsin primary antibody and Alexafluor488 goat-anti-mouse secondary antibody. Mean intensity of Alexafluor-488 as detected by FACS analysis and measured in AU is plotted on the X-axis (determined using Flowing Software, v.2.5.1). By-eye semi-quantitative estimation of Rho expression where P23H was given a rating of “1” (low RHO surface staining) and WT a rating of “3” (normal RHO surface staining) is plotted on the Y-axis. Graphs show a positive correlation between methods.

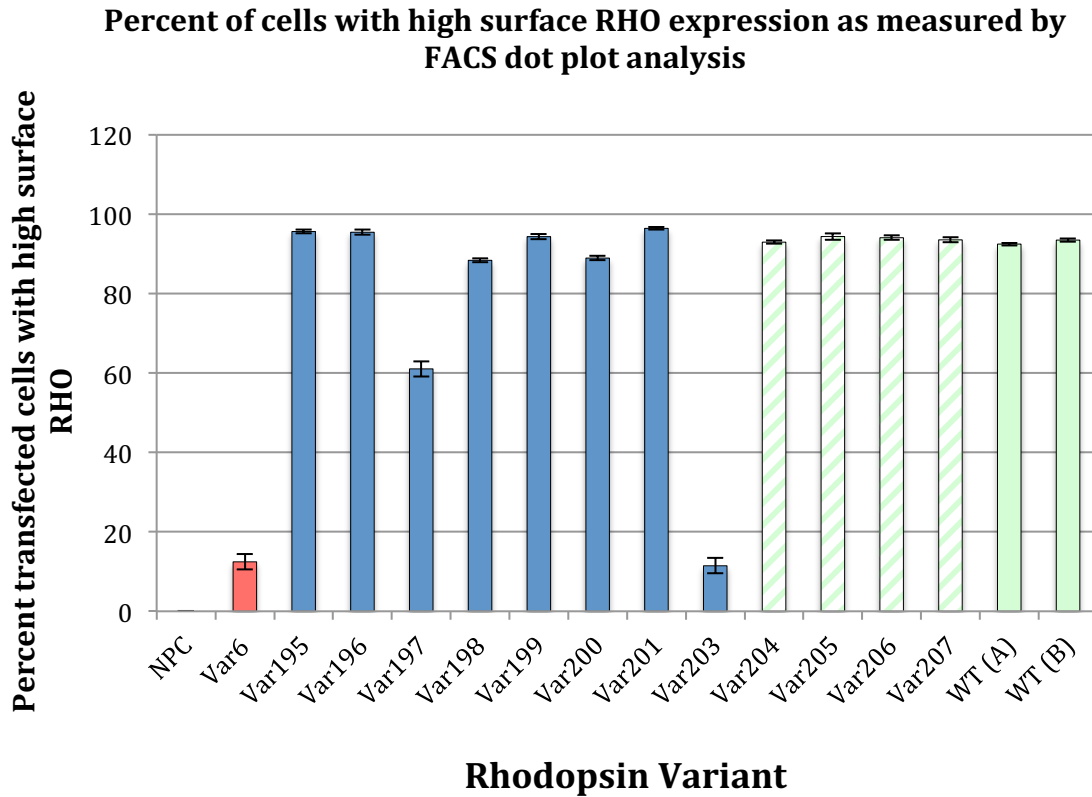


Figure 10. Results of standard FACS assay for variant cohort. Percent of cells with high surface RHO was determined by examining the FACS dot plots of individual transfections. Red Bar: Results from cells transfected with Variant 6, eg. *RHO-P23H*, a known low surface RHO expresser and positive control for the assay. Blue: Cells transfected with *VUS*. Hatched Green: Cells transfected with WT synonymous variants. Solid Green: Cells transfected with *RHO-WT*. A and B have the same sequence but plasmids were prepared on different days as an added control. Standard error is shown for each sample, n=3. Analysis performed with Flowing Software.

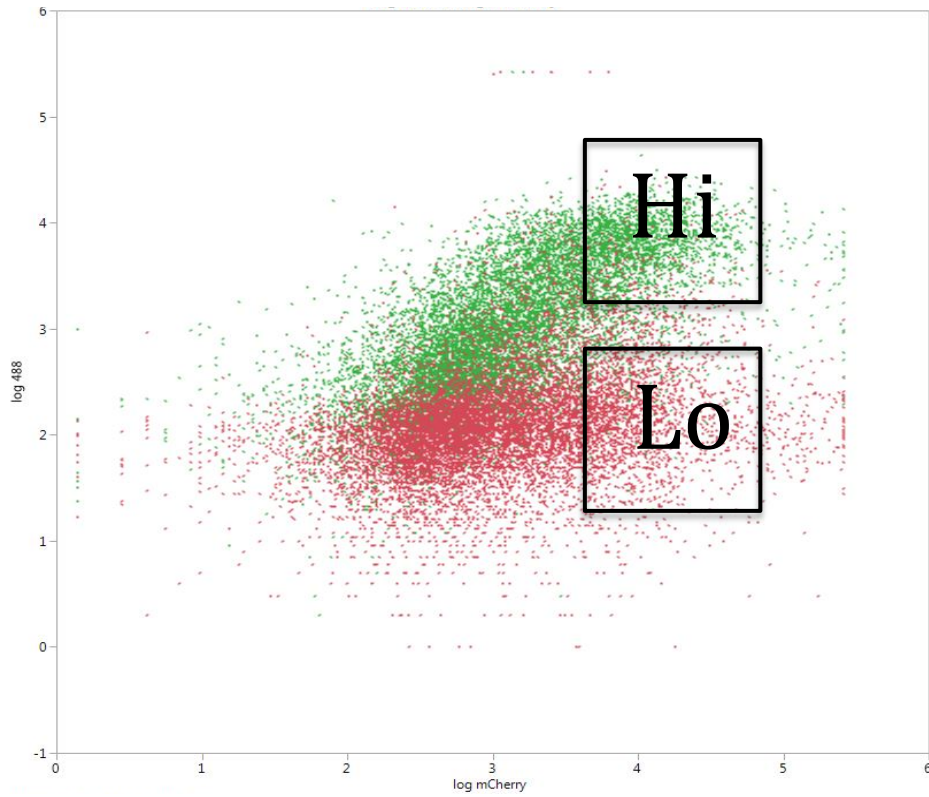


Figure 11. Overlay of standard FACS assay for WT and P23H with gates shown. HEK293 cells were transfected with *RHO-WT* (green) or *RHO-P23H* (red). Sorting gates for transfected cells with high surface RHO (gate “HI”) and low surface RHO (gate “Lo”) were set using these two populations. Overlay created with JMP.

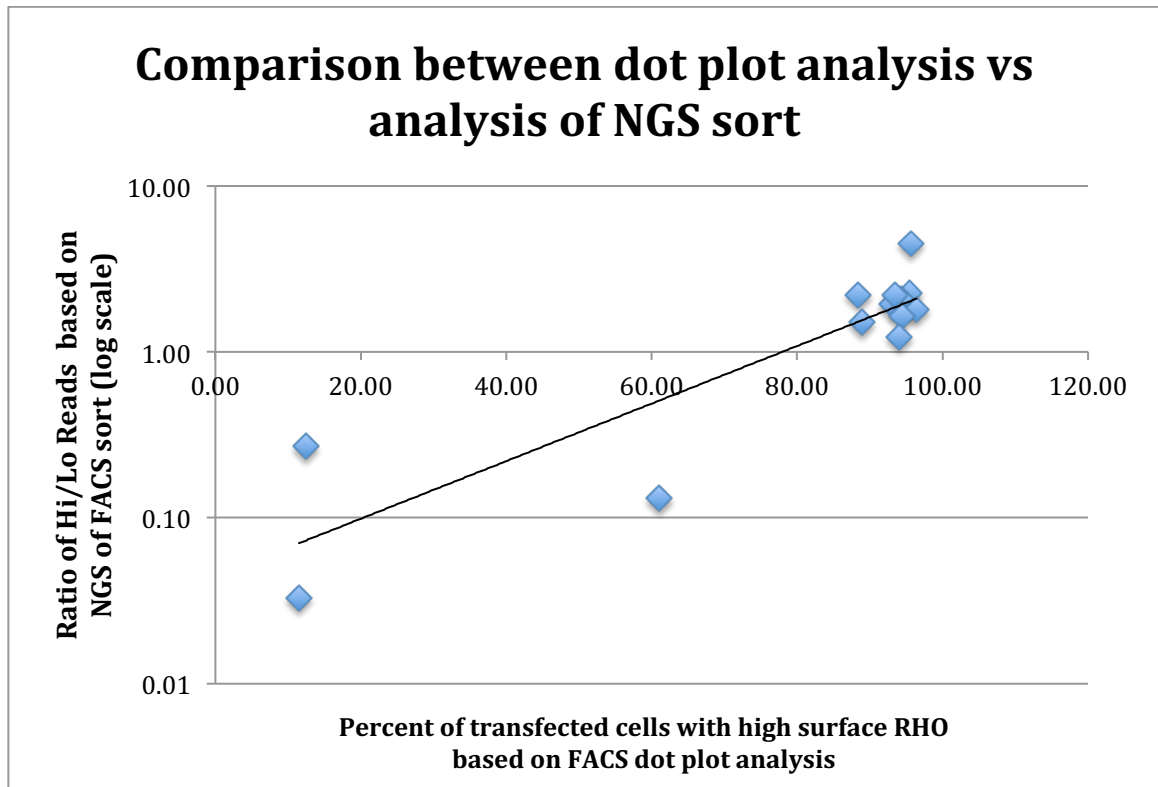


Figure 12. Standard FACS assay correlates with NGS

read analysis of sorted cells. Hi: Population of cells sorted with high levels of Ret-P1 and high levels of mCherry transfection marker. Lo: Population of cells sorted with low levels of Ret-P1 and high levels of mCherry transfection marker. Reads of variants with ratios above 1 are more often found in the Hi group and have a more WT-like phenotype. Reads of variants with ratios below 1 are more often found in the Lo group and have a more P23H-like phenotype.

Variant Number	% of transfected cells with high surface RHO expression (Standard FACS assay)	Rating of Variant as RHO surface expresser (FACS analysis)	NGS analysis of FACS sort; Ratio of Hi/Lo Reads	Rating of Variant as RHO surface expresser (FACS Sort)	Predicted/ Known to be Pathogenic?
6	12.45	Low	0.27	Low	Yes (Known)
195	95.63	High	4.5	High	Unknown
196	95.45	High	2.27	High	Unknown
197	61.04	Intermediate	0.13	Low	Yes (Predicted)
198	88.38	High	2.22	High	Unknown
199	94.33	High	2.07	High	Unknown
200	88.94	High	1.51	High	Unknown
201	96.42	High	1.8	High	Unknown
203	11.46	Low	0.03	Low	Yes (Predicted)
204	92.95	High	1.94	High	No
205	94.36	High	1.64	High	No
206	94.06	High	1.23	High	No
207	93.53	High	2.19	High	No
WT (A)	92.46	High	N/A	High	No (Known)
WT (B)	93.47	High	N/A	High	No (Known)

Table 2. Protein localization assay aids in characterization of *RHO* VUS.

Variants from Table 1 are listed with results of protein localization assay. After standard FACS assay, cells were rated for the level of surface RHO expression as Low, High or Intermediate based on percent of cells with high surface RHO. 0-40% expressers were listed as “Low”, 41-65% “Intermediate” and 66-100% “High”. Cells from the same transfection were fixed with zinc-based fixative (ZBF) and then sorted into two populations of mCherry positive cells: Hi for high Ret-P1 staining and Lo for low Ret-P1 staining. After isolating the plasmid DNA from the sorted populations and amplifying the *RHO* sequences PCR, NGS was performed and the ratio of reads found in the Hi versus Lo group determined for each variant. If the ratio was greater than one, the variant is listed as “High”; if the ratio was less than one, the variant is listed as “Low”. Plasmids which produce a protein which is not expressed on the surface are predicted to be pathogenic. VUS that produce a protein that localizes to the cell surface are not listed as predicted pathogenic, but pathogenicity cannot be ruled out at this point.

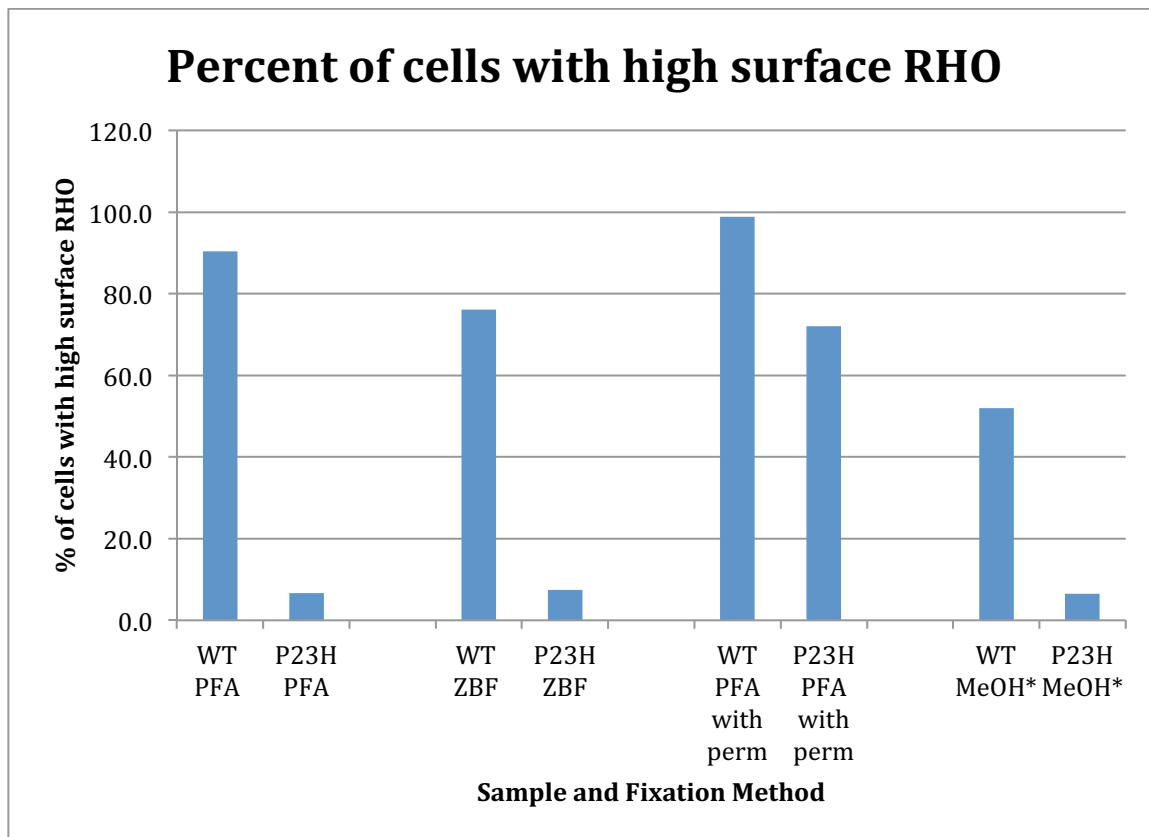


Figure 13. Effect of cell preparation on phenotype readout by FACS. PFA: Paraformaldehyde. ZBF: Zinc-based fixative. PFA with perm: PFA fixation with a permeabilization step with TritonX-100. MeOH: Methanol fixation. *NB: Methanol destroys mCherry fluorescence, so percentage of cells with high surface RHO was determined by dividing % of cells in top two quadrants by the sum of all quadrants. Analysis performed with Flowing Software.

References

- Bainbridge, J. W., Smith, A. J., Barker, S. S., Robbie, S., Henderson, R., Balaggan, K., . . . Ali, R. R. (2008). Effect of gene therapy on visual function in Leber's congenital amaurosis. *N Engl J Med*, *358*(21), 2231-2239. doi: 10.1056/NEJMoa0802268
- Berger, A., Lorain, S., Josephine, C., Desrosiers, M., Peccate, C., Voit, T., . . . Bemelmans, A. P. (2015). Repair of rhodopsin mRNA by spliceosome-mediated RNA trans-splicing: a new approach for autosomal dominant retinitis pigmentosa. *Mol Ther*. doi: 10.1038/mt.2015.11
- Berson, E. L., Rosner, B., Weigel-DiFranco, C., Dryja, T. P., & Sandberg, M. A. (2002). Disease progression in patients with dominant retinitis pigmentosa and rhodopsin mutations. *Invest Ophthalmol Vis Sci*, *43*(9), 3027-3036.
- Braman, J., Papworth, C., & Greener, A. (1996). Site-directed mutagenesis using double-stranded plasmid DNA templates. *Methods in molecular biology* (Clifton, N.J.), *57*, 31-44. doi: 10.1385/0-89603-332-5:31
- Chen, Y., Jastrzebska, B., Cao, P., Zhang, J., Wang, B., Sun, W., . . . Palczewski, K. (2014). Inherent instability of the retinitis pigmentosa P23H mutant opsin. *J Biol Chem*, *289*(13), 9288-9303. doi: 10.1074/jbc.M114.551713
- Daiger, S. P., Sullivan, L. S., & Bowne, S. J. (2013). Genes and mutations causing retinitis pigmentosa. *Clin Genet*, *84*(2), 132-141. doi: 10.1111/cge.12203
- Dellett, M., Sasai, N., Nishide, K., Becker, S., Papadaki, V., Limb, G. A., . . . Ohnuma, S. (2015). Genetic background and light-dependent progression of photoreceptor cell degeneration in prominin-1 knockout mice. *Invest Ophthalmol Vis Sci*, *56*(1), 164-176. doi: 10.1167/iovs.14-15479
- Elachouri, G., Lee-Rivera, I., Clerin, E., Argentini, M., Fridlich, R., Blond, F., . . . Leveillard, T. (2015). Thioredoxin rod-derived cone viability factor protects against photooxidative retinal damage. *Free Radic Biol Med*. doi: 10.1016/j.freeradbiomed.2015.01.003
- Gonzalez-Cordero, A., West, E. L., Pearson, R. A., Duran, Y., Carvalho, L. S., Chu, C. J., . . . Ali, R. R. (2013). Photoreceptor precursors derived from three-dimensional embryonic stem cell cultures integrate and mature within adult degenerate retina. *Nat Biotechnol*, *31*(8), 741-747. doi: 10.1038/nbt.2643
- Hauswirth, W. W., Aleman, T. S., Kaushal, S., Cideciyan, A. V., Schwartz, S. B., Wang, L., . . . Jacobson, S. G. (2008). Treatment of leber congenital amaurosis due to RPE65 mutations by ocular subretinal injection of adeno-associated virus gene

- vector: short-term results of a phase I trial. *Hum Gene Ther*, 19(10), 979-990. doi: 10.1089/hum.2008.107
- Kaushal, S., & Khorana, H. G. (1994). Structure and function in rhodopsin. 7. Point mutations associated with autosomal dominant retinitis pigmentosa. *Biochemistry*, 33(20), 6121-6128.
- Landy, A. (1989). Dynamic, structural, and regulatory aspects of lambda site-specific recombination. *Annual review of biochemistry*, 58, 913-949. doi: 10.1146/annurev.bi.58.070189.004405
- Liang, F. Q., Aleman, T. S., Dejneka, N. S., Dudas, L., Fisher, K. J., Maguire, A. M., . . . Bennett, J. (2001). Long-term protection of retinal structure but not function using RAAV.CNTF in animal models of retinitis pigmentosa. *Mol Ther*, 4(5), 461-472. doi: 10.1006/mthe.2001.0473
- MacLaren, R. E., Groppe, M., Barnard, A. R., Cottrill, C. L., Tolmachova, T., Seymour, L., . . . Seabra, M. C. (2014). Retinal gene therapy in patients with choroideremia: initial findings from a phase 1/2 clinical trial. *Lancet*, 383(9923), 1129-1137. doi: 10.1016/S0140-6736(13)62117-0
- Maguire, A. M., Simonelli, F., Pierce, E. A., Pugh, E. N., Jr., Mingozzi, F., Bencicelli, J., . . . Bennett, J. (2008). Safety and efficacy of gene transfer for Leber's congenital amaurosis. *N Engl J Med*, 358(21), 2240-2248. doi: 10.1056/NEJMoa0802315
- Mao, H., Gorbatyuk, M. S., Rossmiller, B., Hauswirth, W. W., & Lewin, A. S. (2012). Long-term rescue of retinal structure and function by rhodopsin RNA replacement with a single adeno-associated viral vector in P23H RHO transgenic mice. *Hum Gene Ther*, 23(4), 356-366. doi: 10.1089/hum.2011.213
- Marigo, V. (2007). Programmed cell death in retinal degeneration: targeting apoptosis in photoreceptors as potential therapy for retinal degeneration. *Cell Cycle*, 6(6), 652-655.
- McKeone, R., Wikstrom, M., Kiel, C., & Rakoczy, P. E. (2014). Assessing the correlation between mutant rhodopsin stability and the severity of retinitis pigmentosa. *Molecular vision*, 20, 183-199.
- Mendes, H. F., van der Spuy, J., Chapple, J. P., & Cheetham, M. E. (2005). Mechanisms of cell death in rhodopsin retinitis pigmentosa: implications for therapy. *Trends Mol Med*, 11(4), 177-185. doi: 10.1016/j.molmed.2005.02.007
- Meyer, J. S., Howden, S. E., Wallace, K. A., Verhoeven, A. D., Wright, L. S., Capowski, E. E., . . . Gamm, D. M. (2011). Optic vesicle-like structures derived from human pluripotent stem cells facilitate a customized approach to retinal disease treatment. *Stem Cells*, 29(8), 1206-1218. doi: 10.1002/stem.674

- Parmeggiani, F., Sato, G., De Nadai, K., Romano, M. R., Binotto, A., & Costagliola, C. (2011). Clinical and Rehabilitative Management of Retinitis Pigmentosa: Up-to-Date. *Curr Genomics*, *12*(4), 250-259. doi: 10.2174/138920211795860125
- Rana, T., Shinde, V. M., Starr, C. R., Kruglov, A. A., Boitet, E. R., Kotla, P., . . . Gorbatyuk, M. S. (2014). An activated unfolded protein response promotes retinal degeneration and triggers an inflammatory response in the mouse retina. *Cell Death Dis*, *5*, e1578. doi: 10.1038/cddis.2014.539
- Stoletzki, N., & Eyre-Walker, A. (2007). Synonymous codon usage in *Escherichia coli*: selection for translational accuracy. *Molecular biology and evolution*, *24*(2), 374-381. doi: msl166 [pii] 10.1093/molbev/msl166
- Sung, C. H., Davenport, C. M., & Nathans, J. (1993). Rhodopsin mutations responsible for autosomal dominant retinitis pigmentosa. Clustering of functional classes along the polypeptide chain. *J Biol Chem*, *268*(35), 26645-26649.
- Sung, C. H., Schneider, B. G., Agarwal, N., Papermaster, D. S., & Nathans, J. (1991). Functional heterogeneity of mutant rhodopsins responsible for autosomal dominant retinitis pigmentosa. *Proceedings of the National Academy of Sciences of the United States of America*, *88*(19), 8840-8844.
- Tam, B. M., Noorwez, S. M., Kaushal, S., Kono, M., & Moritz, O. L. (2014). Photoactivation-induced instability of rhodopsin mutants T4K and T17M in rod outer segments underlies retinal degeneration in *X. laevis* transgenic models of retinitis pigmentosa. *J Neurosci*, *34*(40), 13336-13348. doi: 10.1523/JNEUROSCI.1655-14.2014
- Wang, D. Y., Chan, W. M., Tam, P. O., Chiang, S. W., Lam, D. S., Chong, K. K., & Pang, C. P. (2005). Genetic markers for retinitis pigmentosa. *Hong Kong Med J*, *11*(4), 281-288.
- Wang, T., & Chen, J. (2014). Induction of the unfolded protein response by constitutive G-protein signaling in rod photoreceptor cells. *J Biol Chem*, *289*(42), 29310-29321. doi: 10.1074/jbc.M114.595207
- Wert, K. J., Lin, J. H., & Tsang, S. H. (2014). General pathophysiology in retinal degeneration. *Dev Ophthalmol*, *53*, 33-43. doi: 10.1159/000357294
- Yang, Y., Mohand-Said, S., Danan, A., Simonutti, M., Fontaine, V., Clerin, E., . . . Sahel, J. A. (2009). Functional cone rescue by RdCVF protein in a dominant model of retinitis pigmentosa. *Mol Ther*, *17*(5), 787-795. doi: 10.1038/mt.2009.28
- Zheng, A., Li, Y., & Tsang, S. H. (2015). Personalized therapeutic strategies for patients with retinitis pigmentosa. *Expert Opin Biol Ther*, *15*(3), 391-402.